Recombination properties of dislocations in GaN

Eugene B. Yakimov,[1,2] Alexander Y. Polyakov,[1] In-Hwan Lee,[3] and Stephen J. Pearton[4,a)]
[1]*National University of Science and Technology MISiS, Moscow 119049, Russia*
[2]*Institute of Microelectronics Technology RAS, Chernogolovka 142432, Russia*
[3]*Department of Materials Science and Engineering, Korea University, Anamro 145, Seoul 02841, South Korea*
[4]*University of Florida, Gainesville, Florida 32611, USA*

(Received 12 July 2017; accepted 20 November 2017; published online 12 December 2017)

The recombination activity of threading dislocations in n-GaN with different dislocation densities and different doping levels was studied using electron beam induced current (EBIC). The recombination velocity on a dislocation, also known as the dislocation recombination strength, was calculated. The results suggest that dislocations in n-GaN giving contrast in EBIC are charged and surrounded by a space charge region, as evidenced by the observed dependence of dislocation recombination strength on dopant concentration. For moderate (below $\sim 10^8\,cm^{-2}$) dislocation densities, these defects do not primarily determine the average diffusion length of nonequilibrium charge carriers, although locally, dislocations are efficient recombination sites. In general, it is observed that the effect of the growth method [standard metalorganic chemical vapor deposition (MOCVD), epitaxial lateral overgrowth versions of MOCVD, and hydride vapor phase epitaxy] on the recombination activity of dislocations is not very pronounced, although the average diffusion lengths can widely differ for various samples. The glide of basal plane dislocations at room temperature promoted by low energy electron irradiation does not significantly change the recombination properties of dislocations. *Published by AIP Publishing*. https://doi.org/10.1063/1.4995580

I. INTRODUCTION

Dislocations in GaN and GaN-based structures are usually present in rather high densities exceeding $10^6\,cm^{-2}$; however, their effect on electrical and optical properties is not fully understood. Dislocations in GaN increase the local nonradiative recombination rate and manifest themselves as dark spots in microcathodoluminescence (MCL) and the electron beam induced current (EBIC) images.[1–4] It has been reported that the diffusion lengths of charge carriers **L** are in anticorrelation with dislocation densities.[4–8] However, quantitatively, such anticorrelation between the dislocation density $\mathbf{N_D}$ and the diffusion length **L** is not well pronounced.[8–10] Moreover, for samples grown by epitaxial lateral overgrowth (ELOG), the dislocation densities in the wing and gap regions differ by about two orders of magnitude, while the difference in the diffusion length is at most a factor of 2–3, and in many structures, the diffusion lengths are the same in the high-dislocation-density gaps and low-dislocation density wings.[11–13] Direct estimations also show that the dislocation density is not the main factor limiting the diffusion length in GaN.[10] The results of the diffusion length measurements in GaN with different dislocation densities are shown in Fig. 1. The dotted line shows the **L** dependence on N_D calculated under the assumption that dislocations decrease the effective (measured) diffusion length by 10%, relative to its value in dislocation-free region. Most points are below or close to this line, which means that the dislocations effect on the effective diffusion length is low. Therefore, point defects have been assumed to limit the diffusion length value.[14–17] However, dislocations have been shown to enhance carrier transport across the active layer of light emitting diodes (LEDs),[18] to adversely affect the parameters of high electron mobility transistors (HEMTs)[19–21] and can accelerate degradation of LEDs and laser diodes (LDs).[22] Therefore, understanding the nature of dislocation recombination activity is still important from both fundamental and practical points of view and could help to guide device improvements.

The majority of theoretical and experimental investigations show that screw and mixed threading dislocations introduce both deep and shallow gap states, i.e., the activity of at least screw and mixed threading dislocations can be intrinsic.[23,24] Numerous investigations by the electron holography,[25,26] EELS,[27] and scanning probe microscopy methods[28] indicate that the charge in the dislocation core can be up to 4×10^7 e/cm. On the other hand, point defect atmospheres, in particular, oxygen segregation on dislocations and vacancy type, defect decoration of dislocations were also suggested.[28–30] Thus, up till now, it is not clear if the nature of dislocation activity in GaN is intrinsic or it is determined by point defect gettering. Understanding this point opens ways to control the dislocation properties and their effects on device performance. It is useful to compare the recombination activity of dislocations in crystals grown by different methods and containing different dislocation densities because the relative effect of gettering should increase with the impurity content increase and/or with a decrease of the dislocation density.

II. EXPERIMENTAL

The n-GaN samples used were grown by standard metalorganic chemical vapor deposition (MOCVD), by ELOG, by pendeo epitaxy (a version of epitaxial lateral overgrowth)

a)Author to whom correspondence should be addressed: spear@mse.ufl.edu

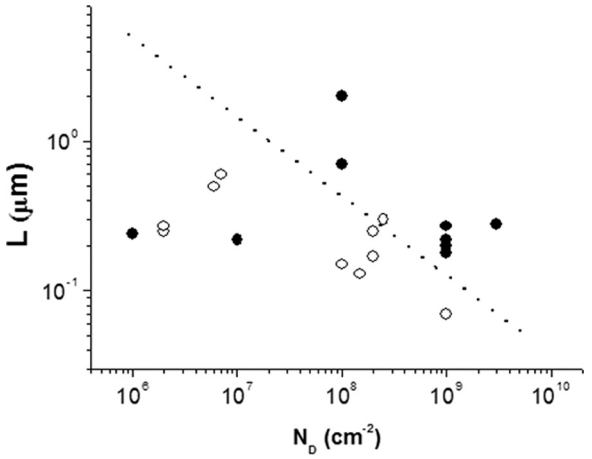

FIG. 1. $\mathbf{L}(\mathbf{N_D})$ dependence. Our results are shown with open circles and previously reported[5,6,8] by filled ones. The dotted line shows the $\mathbf{L}(\mathbf{N_D})$ dependence on N_D calculated under assumption of 10% dislocation effect.

and by hydride vapor phase epitaxy (HVPE) methods. Their details were reported elsewhere.[4,12,13,15,17,31,32] MOCVD films were prepared on c-plane sapphire substrates by metal-organic chemical vapor deposition (MOCVD) (Veeco D180 GaN). The sapphire substrates were preheated to 1080 °C in hydrogen ambient for 6 min to remove any surface contamination. A low temperature GaN nucleation layer with thickness of 30 nm was deposited at 540 °C. Nominally undoped or lightly Si doped n-GaN films with thickness of several microns were grown at 1054 °C. Trimethylgallium and ammonia (NH_3) were used as Ga and N precursors, while silane (SiH_4) was the n-type dopant.

ELOG films were prepared by the lateral overgrowth over SiO_2 stripes deposited on GaN MOCVD template prepared as mentioned earlier. The stripes width was 12 μm, the window between the stripes was 4 μm, the stripes direction was [1–100], the thickness of the MOCVD template was 2 μm, the thickness of the ELOG films was between 6 and 12 μm. ELOG samples were either unintentionally doped n-type or lightly n-type doped by Si.

Pendeo epitaxy is the mirror version of the lateral overgrowth method in ELOG. In pendeo samples, trenches were prepared in the MOCVD GaN template by dry etching via a Ni etch mask deposited on the template using an e-beam evaporator. A mask pattern consisting of Ni stripes of 4 μm width separated by 14 μm gaps and going in the [1–100] direction was prepared by negative photolithography and reactive ion etching. After the photoresist lift-off, the n-GaN template (thickness of 1 μm) was etched off in the gaps of the mask down to sapphire using inductively coupled plasma (ICP) dry etching. Thus, a patterned n-GaN template with 14 μm trenches and 4 μm ridges (seeds) was formed for subsequent selective regrowth.

These n-GaN templates were then reloaded into the MOCVD chamber for pendeo epitaxial lateral overgrowth. The lateral overgrowth was achieved within the temperature range of 1050–1085 °C using a pressure of 300 Torr. The thickness of this well coalesced undoped layer was close to 6 μm. Pendeo films were either unintentionally doped or lightly Si doped. Bulk HVPE samples were acquired from Kyma Technologies (USA). These were unintentionally n-type doped wafers sliced from HVPE boules grown in the [0001] direction, polished on the Ga side and cut into 1 cm^2 square pieces (the thickness was close to 450 μm).

The films and HVPE crystals were processed into Schottky diodes with diameter close to 1 mm by thermal evaporation through a shadow mask. The dislocation densities were determined by counting the dark spot defects in electron beam induced current (EBIC) images or microcathodoluminescence (MCL) images.[1,3] The net donor concentrations were obtained from capacitance-voltage C-V profiling performed on multiple Schottky diodes.[14,17] C-V probing is preferable to Hall measurements in this case because of the impact in the latter case of highly conducting layers near the interface with the substrate.[33,34]

The diffusion lengths L_d were calculated by fitting the dependence of EBIC collection efficiency on the beam accelerating voltage.[9] This fitting procedure also yields the local net donor (or acceptor) doping in the spot probed by EBIC by providing the local thickness of the space charge region and the local conductivity type.[9–12,17,32] For MOCVD and HVPE samples studied in this work, no serious lateral non-uniformity of donor concentration measured by C-V profiling on multiple Schottky diodes was observed, and the results of net donor concentration obtained from C-V profiling and from EBIC fitting were reasonably close verifying the validity of the latter approach. This is important because, for ELOG and pendeo films, the growth mode of the laterally overgrown low-dislocation-density wing regions is different from the growth mode in the windows/seeds high-dislocation density regions. This can easily result in different donor incorporation efficiencies and different local net donor concentrations in the wing and windows/seeds regions.[33–35] Therefore, local doping characterization techniques, such as the scanning capacitance microscopy (SCM)[33] or the EBIC-based method,[9–12,32] should be used. The latter approach applied to ELOG and pendeo films described earlier showed that, for undoped pendeo samples in our experiments, the wing regions had low n-type conductivity, whereas the seed regions were lightly p-type,[32] as evident from the sign of the EBIC current at 0 V bias. Light n-type doping leveled-off the donor densities in both regions of pendeo samples and yielded concentrations close to the C-V profiling results obtained on Schottky diodes.[32] For ELOG samples under our growth conditions, the donor concentrations in the wings were always several times lower than in the windows,[11,12] irrespective of whether the films were unintentionally doped or undoped. Table I summarizes the data on donor densities and diffusion lengths obtained from EBIC experiments for undoped HVPE and lightly n-type doped pendeo samples, and for the two regions of the undoped (ELOG1) and lightly n-type doped ELOG2-ELOG4 samples.

The dislocation density, diffusion length, and donor concentration were varied in the range from 10^6 to 2×10^9 cm^{-2}, from 90 to 600 nm, and from 7×10^{15} to 4×10^{17} cm^{-3}, respectively. The ELOG structures employed have very similar diffusion lengths but different dopant concentrations. What is especially important is that the dopant concentration in the wing and gap regions differs at least by 2–3 times.[11,12]

TABLE I. Parameters of structures studied and the results obtained.

	L (nm)	N_d ($\times 10^{17}$ cm^{-3})	C (%)	γ_1	γ_{corr} (cm^2/s)
MOCVD1	90	4	14	0.9	0.53
MOCVD2	260	0.4	9	0.8	1.5
ELOG1window	260	1	18	1.8	2.13
ELOG1wing	260	0.4	12	1.6	3
HVPE	500	0.55	16	1.6	2.56
ELOG2 window	204	0.8	8	0.8	1.06
ELOG2 wing	240	0.2	6	1	2.65
ELOG3 window	240	1.5	8	0.4	0.39
ELOG3 wing	240	0.5	7	0.5	0.84
ELOG4 window	260	0.35	15	2.2	4.4
ELOG4 wing	260	0.07	10	9.8	44
Pendeo-seed and wing	50	4	13	9	10.65

The dislocation structure of the studied pendeo samples was very similar to ELOG, but showed a much higher concentration of deep traps and much lower diffusion lengths, although the difference between the diffusion lengths in the low-dislocation-density wings and high-dislocation-density seeds was as negligible as for ELOG.[14]

The dislocation density was obtained from the electron beam induced current (EBIC) images, and therefore, only electrically and recombination active dislocations were counted. The Schottky barriers necessary for the EBIC measurements were prepared by Au evaporation. The EBIC measurements were carried out in a JSM-840 scanning electron microscope at room temperature. A beam current of 10^{-10} A was used for most of the measurements. The diffusion length **L** and depletion region width **W** values were obtained by fitting the experimental dependences of the collected current in the EBIC mode on beam energy $\mathbf{E_b}$ to modeling results (see Refs. 9–12 and references therein). For GaN, this approach was verified in Ref. 11 by a comparison of EBIC and C-V measurement results and in Ref. 9 by the measurements of diffusion length in the same samples by different methods. The dislocation contrast, as usual, was calculated as $\mathbf{C(r)} = 1 - \mathbf{I_c(r)/I_0}$, where $\mathbf{I_c(r)}$ is the collected current for e-beam located at a distance **r** from a dislocation and $\mathbf{I_0}$ is the collected current far from the dislocation in the dislocation-free region. In the present paper, only the maximum EBIC contrast **C**(0) was considered. The dislocation contrast measurements were carried out at beam energy $E_b = 35$ keV because the dislocation contrast width in GaN decreases, and therefore the lateral resolution improves with the $\mathbf{E_b}$ increase.[4] Indeed, such energy allows to reveal individual dislocations even when their density exceeds 10^8 cm^{-2} (Fig. 2). To calculate the average contrast, at least 10 dislocations for all samples were used.

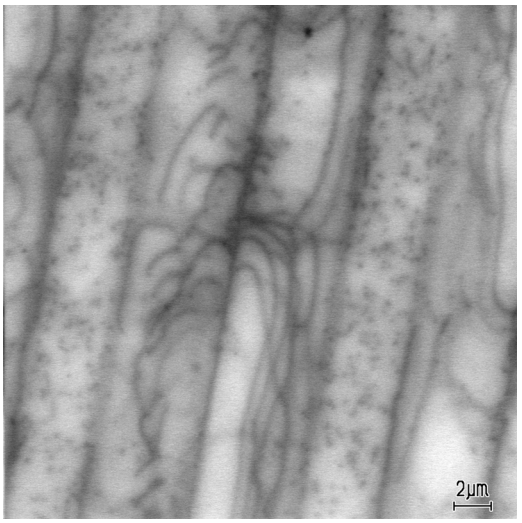

FIG. 2. EBIC image of 6 μm thick ELOG GaN film. Threading dislocations with $\mathbf{N_D}$ about 10^8 cm^{-2} can be seen in the slit regions as dark spots while few threading and basal dislocations can be seen in the wing regions.

The nature of residual donors and major compensating centers in our samples, based on previous studies[14–17,22] show the residual donors in MOCVD, ELOG, pendeo, and HVPE samples are oxygen and Si, while the compensating acceptors come from deep traps, some of which are due to carbon and others due to gallium vacancy complexes with shallow dopants.

III. RESULTS AND DISCUSSION

The dislocation contrast itself cannot be used for characterization of dislocation activity because it depends on beam energy, depletion region width, and diffusion length. For this purpose, the dislocation recombination strength γ (the recombination velocity on a dislocation)[36] should be used. The value of γ was obtained from a comparison of measured and calculated dislocation EBIC contrast. The dislocation contrast was calculated as[36]

$$\mathbf{C}(0) = \frac{\frac{2}{\pi}\int_{\mathbf{W}}^{\infty}\int_{0}^{\infty}\int_{0}^{\infty}\frac{\frac{\boldsymbol{\gamma}}{\mathbf{D}}\frac{\mathbf{k}}{\boldsymbol{\mu}^2}\mathbf{r}}{1+\frac{\boldsymbol{\gamma}}{\boldsymbol{\pi}\mathbf{D}\boldsymbol{\mu}^2\mathbf{r_d^2}}[1-\boldsymbol{\mu}\mathbf{r_d}\mathbf{K}_1(\boldsymbol{\mu}\mathbf{r_d})]}\mathbf{K}_0(\boldsymbol{\mu}\mathbf{r})\sin(\mathbf{kz})\mathbf{g}(\mathbf{z},\mathbf{r})\mathbf{dk}\mathbf{dr}\mathbf{dz}}{\mathbf{I_0}}, \quad (1)$$

where **D** is the excess carrier diffusivity, $\boldsymbol{\mu} = \mathbf{k}^2 + 1/\mathbf{L}^2$, K_0 and K_1 are the modified Bessel functions of order zero and one, respectively, $\mathbf{r_d}$ is the radius of dislocation defect cylinder, which in our calculations is assumed to be equal to 50 nm, and $\mathbf{g(z,r)}$ is the function describing the generation rate distribution. It should be noted that the chosen value for $\mathbf{r_d}$ is close to that obtained by fitting the dislocation contrast profile.[37] Besides, as shown in Refs. 3 and 38, the contrast

dependence on $\mathbf{r_d}$ is rather weak. The depth dependence of $\mathbf{g(z,r)}$ for GaN was derived in Ref. 39. However, the radial distribution was not obtained previously. Therefore, the empirical expression for radial distribution is obtained by fitting the distributions calculated by the Monte Carlo Casino program for a few beam energy values. As a result, $\mathbf{g(z,r)}$ can be described as

$$\mathbf{g(z,r)} = \frac{3.207}{2\pi\boldsymbol{\sigma}^2\mathbf{R_{Beth}}}\mathbf{exp}\left[-\mathbf{A}(\mathbf{z}/\mathbf{R_{Beth}} - 0.11)^2\right]\mathbf{exp}(-\mathbf{r}^2/2\boldsymbol{\sigma}^2), \tag{2}$$

where $\mathbf{R_{Beth}}\ (\mu\mathrm{m}) = 0.0132\cdot\mathbf{E_b}\ (\mathrm{keV})^{1.75}$ is the electron Bethe range, $\mathbf{A} = \begin{cases} 42.8, \mathbf{z} < 0.11\cdot\mathbf{R_{Beth}} \\ 16.5, \mathbf{z} \geq 0.11\cdot\mathbf{R_{Beth}} \end{cases}$,[39] $\sigma = (0.1*\mathbf{d}^2 + 2\mathbf{z}^3/\mathbf{R_{Beth}}/(1+50\exp(-z/0.03/\mathbf{R_{Beth}})))^{1/2}$, and $\mathbf{d}$ is the beam diameter. As seen in (1), the contrast $\mathbf{C}$ depends on the relation $\gamma/\mathbf{D}$. Therefore, it is useful to introduce the normalized strength $\gamma_1 = \gamma/\mathbf{D}$ because of a considerable amount of disagreement regarding the reported $\mathbf{D}$ values in the literature. It should be stressed that just γ_1 value can be obtained by contrast fitting.

The results of dislocation contrast measurements in the structures studied and the corresponding γ_1 values obtained by their fitting using (1) are presented in Table I. In most structures the calculated γ_1 values fall within the range from 0.5 to 2. At first glance, it could be assumed that the dislocation recombination strength depends on the growth method. Thus, in the structures grown by the MOCVD, in spite of the difference in the diffusion length and dopant concentration, γ_1 values are practically the same and are close to the values previously obtained on the MOCVD structures.[3,4] By contrast, the diffusion length and the dopant concentration in MOCVD2 and in the wings of ELOG1 are practically the same but the γ_1 value in the first structure is two times smaller than in the second. However, a pronounced difference between γ_1 values in different ELOG structures can be seen. An analysis of the results obtained does not reveal any correlation between the diffusion length and the dislocation recombination strength. However, a comparison of ELOG structures having practically the same diffusion length but different dopant concentrations in the wing and window regions shows that γ_1 probably depends on the dopant concentration. The real dislocation activity is determined by the γ value, which is equal to γ_1 at $\mathbf{D} = 1\ \mathrm{cm}^2/\mathrm{s}$. In general, the ambipolar diffusivity should be used in expression (1), but at low excitation level, it is equal to the minority carrier (hole) diffusivity. The hole diffusivity $\mathbf{D}$ can be obtained from the hole mobility μ using the Einstein relation $\mathbf{D} = \frac{\mu\mathbf{k_B}\mathbf{T}}{\mathbf{e}}$, where $\mathbf{k_B}$ is the Boltzmann's constant and T is the temperature. However, a considerable spread regarding the reported mobility values exists in the literature. Thus, for low-doped GaN a value of about $200\ \mathrm{cm}^2\ \mathrm{V}^{-1}\mathrm{S}^{-1}$ is quoted in Ref. 40, while in Ref. 41 it was only $40\ \mathrm{cm}^2\ \mathrm{V}^{-1}\mathrm{s}^{-1}$. At room temperature that gives $\mathbf{D}$ equal to 5 and $1\ \mathrm{cm}^2/\mathrm{s}$, respectively. In both papers, the mobility and accordingly the diffusivity decreases with the acceptor concentration $\mathbf{N_a}$. The dependence can be approximated from the data presented in Ref. 40 as $\mathbf{D} = 3.75\times10^8/(\mathbf{N_a})^{1/2}\ \mathrm{cm}^2/\mathrm{s}$. In n-GaN, the $\mathbf{D}$ dependence on donor concentration $\mathbf{N_d}$ can differ from that in p-GaN; however, under an assumption that it is the same, the correction of γ value on $\mathbf{D}(\mathbf{N_d})$ can be made. In Fig. 3, these corrected γ values together with those calculated with constant $\mathbf{D} = 1\ \mathrm{cm}^2/\mathrm{s}$ (equal to γ_1) are presented as a function of donor concentration. The γ_1 increase with $\mathbf{N_d}$ decreasing can be seen, and after the correction, the increase becomes even more pronounced. γ can be expressed as $\boldsymbol{\gamma} = \frac{\pi\mathbf{r_d^2}}{\tau} = \pi\mathbf{r_d^2}\mathbf{v_{th}}\boldsymbol{\sigma_d}\mathbf{N} = \mathbf{v_{th}}\boldsymbol{\sigma_d}\mathbf{N_l}$, where $\mathbf{v_{th}}$ is the thermal velocity, $\boldsymbol{\sigma}$ and $\mathbf{N}$ are the capture cross-section and density of traps inside the dislocation cylinder, respectively, and $\mathbf{N_l}$ is the line density of defects along the dislocations. Assuming for σ values about 10^{-15}–$10^{-14}\ \mathrm{cm}^2$, $\mathbf{N_l}$ can be estimated. That gives the values in the range from 3×10^6 to $3\times10^8\ \mathrm{cm}^{-1}$ that correlates well with the trap density obtained from the measured dislocation charge.[26,27]

Thus, it seems that the γ values decrease with the increase in $\mathbf{N_d}$. The calculation approach used assumes that the dislocation is not charged and that its contrast inside the depletion region is negligible. If dislocations in GaN are charged and preserve this charge under the e-beam excitation, the radius of depletion region around dislocations increases with the decrease in $\mathbf{N_d}$. That should lead to the increase in contrast. Besides, with the decrease in $\mathbf{N_d}$, the electric field inside the Schottky barrier depletion region decreases and the recombination on dislocations inside the depletion region cannot be totally excluded. Thus, the assumption about the dislocation charge allows at least partially to explain the dependence of dislocation activity on dopant concentration. A comparison of results obtained on the structures ELOG1 and ELOG3 shows that in the structures with similar parameters, the values of γ can significantly differ. This could mean that not only donors but also other impurities can affect the dislocation activity. It cannot be also totally excluded that point defects affect the diffusion coefficient $\mathbf{D}$ value but not the dislocation recombination strength. Thus, although the theory predicts that the screw and mixed threading dislocations should have intrinsic deep levels and that the recombination activity of dislocations can be intrinsic in nature, in real structures, the recombination activity of threading dislocations seems to depend at least in some cases on its interaction with point defects. This could open ways for controlling the dislocation in the electrical properties.

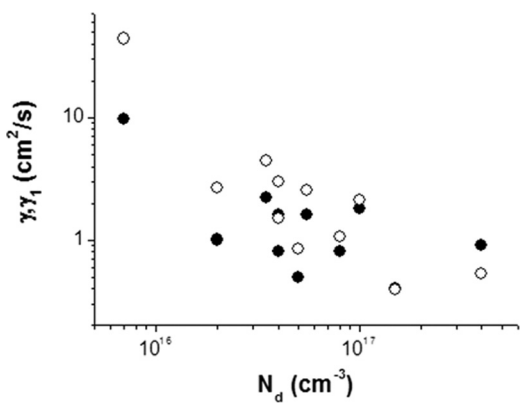

FIG. 3. Dependence of corrected γ (open symbols) and γ_1 (filled symbols) on dopant concentration.

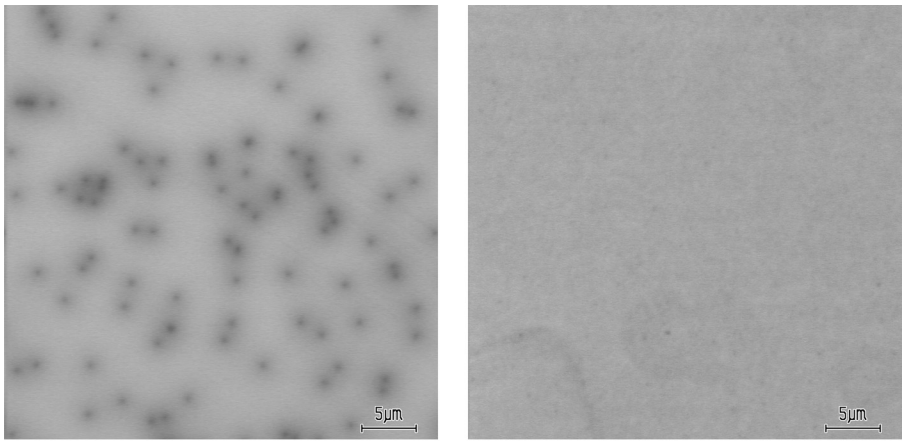

FIG. 4. EBIC images of HVPE samples before (a) and after 6 MeV electron irradiation up to the dose of 10^{16} cm^{-2} (b).

There is still more to understand about the observed phenomena. For example, in the study of effects in HVPE GaN irradiated with 6 MeV electrons, we observed that after a dose of $\sim 10^{16}$ cm^{-2}, the net donor concentration decreased from 5×10^{16} cm^{-3} to 1.2×10^{16} cm^{-3} and the diffusion length was reduced to 95 nm from the original value of 600 nm. Correspondingly, the dislocation EBIC contrast decreased from about 16% to less than 1%, so that dislocations practically could not be resolved in the EBIC mode (Fig. 4). One possibility is that, as the result of irradiation, the concentration of deep recombination centers increases, which causes the decrease of diffusion length and, thus, of the dislocation contrast. The argument against it is that we can easily observe dislocations with high EBIC contrast in MOCVD or pendeo samples with similarly low diffusion lengths. The explanation in that case could be that the concentration and type of deep traps in the matrix and on dislocations in HVPE GaN are quite different as compared to MOCVD or pendeo GaN. This is indeed the case.[14–16] In HVPE material, the density of all electron traps is very low. After irradiation, the main effect is the strong increase in the density of the E_c–1 eV centers that seem to be responsible for the nonradiative recombination of charge carriers.[17] In MOCVD and pendeo samples with low diffusion length, the dominant recombination centers are the E_c–0.56 eV traps while the density of the E_c–1 eV traps is quite low. The suggestion is that the traps decorating dislocations in HVPE are similar to the E_c–1 eV traps. Alternately, it could be assumed that electron irradiation dissociates some preexisting defects, for example, hydrogen-related defects and releases hydrogen or other mobile defects at room temperature. Gettering of such mobile defects on dislocations could then passivate their electrical activity. The density of the E_c–0.56 eV recombination centers is not seriously altered by electron irradiation.[17] To check which of the scenarios is true, one could look at the dislocation contrast in irradiated MOCVD or pendeo GaN.

All previous results are related to threading dislocations. The intrinsic activity of basal screw dislocations was shown to be lower than that of screw threading dislocations.[42] Nevertheless, they produce noticeable contrast in ELOG GaN in EBIC mode (Fig. 2). The segments of these basal screw dislocations in ELOG wings can move with a velocity of about 10 nm/s under the SEM probing beam.[43,44] This was ascribed to the recombination enhanced dislocation glide (REDG). This REDG-induced dislocation glide, however, was not accompanied by measurable changes in dislocation contrast (Fig. 5). One has to assume, then, that either the recombination activity of basal screw dislocations in n-GaN is intrinsic or that the defects decorating the dislocations and accounting for the recombination activity are mobile at room temperature, and can follow the movement of the dislocation core.

IV. CONCLUSIONS

The recombination activity of dislocations in GaN grown by different methods, and containing different dislocation densities and dopant concentrations, has been studied by EBIC. The strong dependence of dislocation recombination strength on dopant concentration could indicate that dislocations visible in EBIC in n-GaN are charged and surrounded by space charge regions. No obvious correlation

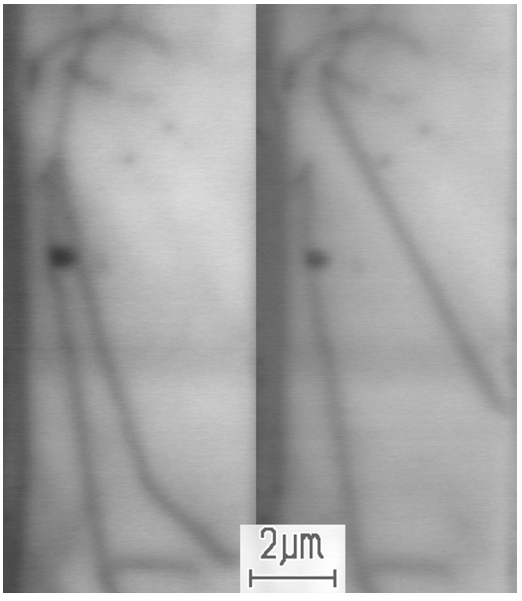

FIG. 5. EBIC images of basal dislocations in ELOG GaN before (left) and after e-beam irradiation at 35 keV up to a dose of 10^{-2} C/cm^2.

between the dislocation activity, the diffusion length, and the growth method was observed. The dislocation recombination activity can be modulated by its interaction with point defects, and, in particular, the electron irradiation can essentially suppress it. The glide of basal dislocations at room temperature under low energy electron irradiation does not change the recombination properties, suggesting that either the recombination activity of such dislocations is intrinsic in nature or that the defects decorating these dislocations are mobile at room temperature and can follow the movement of the core.

ACKNOWLEDGMENTS

The work at NUST MISiS was supported in part by the Ministry of Education and Science of the Russian Federation in the framework of the Increase Competitiveness Program of NUST(MISiS) (No. K2-2014-055). The work at the Korea University was supported by the National Research Foundation of Korea (NRF) funded by the Ministry of Science, ICT and Future Planning (No. 2017R1A2B3006141). The work at UF was supported by DTRA Grant No. HDTRA1-17-1-0011.

[1]1. S. J. Rosner, E. C. Carr, M. J. Ludowise, G. Girolami, and H. I. Erikson, Appl. Phys. Lett. **70**, 420 (1997).
[2]S. C. Jain, M. Willander, J. Narayan, and R. Van Overstraeten, J. Appl. Phys. **87**, 965 (2000).
[3]E. B. Yakimov, J. Phys.: Condens. Matter **14**, 13069 (2002).
[4]N. M. Shmidt, O. A. Soltanovich, A. S. Usikov, E. B. Yakimov, and E. E. Zavarin, J. Phys.: Condens. Matter **14**, 13285 (2002).
[5]P. M. Bridger, Z. Z. Bandić, E. C. Piquette, and T. C. McGill, Appl. Phys. Lett. **73**, 3438 (1998).
[6]L. Chernyak, A. Osinsky, G. Nootz, A. Schulte, J. Jasinski, M. Benamara, Z. Liliental-Weber, D. C. Look, and R. J. Molnar, Appl. Phys. Lett. **77**, 2695 (2000).
[7]O. A. Soltanovich, E. B. Yakimov, N. M. Shmidt, A. S. Usikov, and W. V. Lundin, Physica B **340–342**, 479 (2003).
[8]K. Kumakura, T. Makimoto, N. Kobayashi, T. Hashizume, T. Fukui, and H. Hasegawa, Appl. Phys. Lett. **86**, 052105 (2005).
[9]E. B. Yakimov, J. Alloys Compd. **627**, 344 (2015).
[10]E. B. Yakimov, Jpn. J. Appl. Phys., Part 1 **55**, 05FH04 (2016).
[11]E. B. Yakimov, P. S. Vergeles, A. Y. Polyakov, N. B. Smirnov, A. V. Govorkov, I.-H. Lee, C. R. Lee, and S. J. Pearton, Appl. Phys. Lett. **90**, 152114 (2007).
[12]E. B. Yakimov, P. S. Vergeles, A. Y. Polyakov, N. B. Smirnov, A. V. Govorkov, I.-H. Lee, C. R. Lee, and S. J. Pearton, Appl. Phys. Lett. **92**, 042118 (2008).
[13]A. Y. Polyakov, N. B. Smirnov, A. V. Govorkov, A. V. Markov, E. B. Yakimov, P. S. Vergeles, I.-H. Lee, C. R. Lee, and S. J. Pearton, J. Vac. Sci. Technol. B **26**, 990 (2008).
[14]I.-H. Lee, A. Y. Polyakov, N. B. Smirnov, E. B. Yakimov, S. A. Tarelkin, A. V. Turutin, I. V. Shemerov, and S. J. Pearton, Appl. Phys. Express **9**, 061002 (2016).
[15]I.-H. Lee, A. Y. Polyakov, N. B. Smirnov, E. B. Yakimov, S. A. Tarelkin, A. V. Turutin, I. V. Shemerov, and S. J. Pearton, J. Appl. Phys. **119**, 205109 (2016).
[16]A. Y. Polyakov, N. B. Smirnov, E. B. Yakimov, S. A. Tarelkin, A. V. Turutin, I. V. Shemerov, S. J. Pearton, K.-B. Bae, and I.-H. Lee, J. Alloys Compd. **686**, 1044 (2016).
[17]I.-H. Lee, A. Y. Polyakov, E. B. Yakimov, N. B. Smirnov, I. V. Shchemerov, S. A. Tarelkin, S. I. Didenko, K. I. Tapero, R. A. Zinovyev, and S. J. Pearton, Appl. Phys. Lett. **110**, 112102 (2017).
[18]N. M. Shmidt, P. S. Vergeles, and E. B. Yakimov, Semiconductors **41**, 491 (2007).
[19]A. Hinoki, J. Kikawa, T. Yamada, T. Tsuchiya, S. Kamiya, M. Kurouchi, K. Kosaka, T. Araki, A. Suzuki, and Y. Nanishi, Appl. Phys. Express **1**, 011103 (2008).
[20]J. J. M. Law, E. T. Yu, G. Koblmüller, F. Wu, and J. S. Speck, Appl. Phys. Lett. **96**, 102111 (2010).
[21]F. Gao, B. Lu, L. Li, S. Kaun, J. S. Speck, C. V. Thompson, and T. Palacios, Appl. Phys. Lett. **99**, 223506 (2011).
[22]A. Y. Polyakov and I.-H. Lee, Mater. Sci. Eng., R **94**, 1 (2015).
[23]L. Lymperakis, J. Neugebauer, M. Albrecht, T. Remmele, and H. P. Strunk, Phys. Rev. Lett. **93**, 196401 (2004).
[24]I. Belabbas, J. Chen, and G. Nouet, Phys. Status Solidi C **12**, 1123–1128 (2015).
[25]C. Jiao and D. Cherns, J. Electron Microsc. **51**, 105 (2002).
[26]E. Müller, D. Gerthsen, P. Brückner, F. Scholz, T. Gruber, and A. Waag, Phys. Rev. B **73**, 245316 (2006).
[27]I. Arslan, A. Bleloch, E. A. Stach, S. Ogut, and N. D. Browning, Philos. Mag. **86**, 4727 (2006).
[28]A. Krtschil, A. Dadgar, and A. Krost, J. Cryst. Growth **248**, 542 (2003).
[29]I. Arslan and N. D. Browning, Phys. Rev. Lett. **91**, 165501 (2003).
[30]M. E. Hawkridge and D. Cherns, Appl. Phys. Lett. **87**, 221903 (2005).
[31]N. M. Shmidt, V. V. Sirotkin, A. A. Sitnikova, O. A. Soltanovich, R. V. Zolotareva, and E. B. Yakimov, Phys. Status Solidi C **2**, 1797 (2005).
[32]A. Y. Polyakov, N. B. Smirnov, E. B. Yakimov, I.-H. Lee, and S. J. Pearton, J. Appl. Phys. **119**, 015103 (2016).
[33]T. Zhu and R. A. Oliver, Phys. Chem. Chem. Phys. **14**, 9558 (2012).
[34]T. Zhu, C. F. Johnston, M. Häberlen, M. J. Kappers, and R. A. Oliver, J. Appl. Phys. **107**, 023503 (2010).
[35]J. Sumner, S. Das Bakshi, R. A. Oliver, M. J. Kappers, and C. J. Humphreys, Phys. Status Solidi B **245**, 896 (2008).
[36]C. Donolato, J. Appl. Phys. **84**, 2656 (1998).
[37]C. A. Donolato, Semicond. Sci. Technol. **7**, 37 (1992).
[38]E. B. Yakimov, S. S. Borisov, and S. I. Zaitsev, Semiconductors **41**, 411 (2007).
[39]D. K. Gaskill, L. B. Rowland, and K. Doverspike, "Electrical transport properties of A1N, GaN and AlGaN," in *Properties of Group III Nitrides*, edited by J. Edgar (INSPEC, 1994), pp. 101–116.
[40]Y. Arakawa, K. Ueno, A. Kobayashi, J. Ohta, and H. Fujioka, APL Mater. **4**, 086103 (2016).
[41]I. Belabbas, J. Chen, M. I. Heggie, C. D. Latham, M. J. Rayson, P. R. Briddon, and G. Nouet, Modell. Simul. Mater. Sci. Eng. **24**, 075001 (2016).
[42]E. B. Yakimov, P. S. Vergeles, A. Y. Polyakov, I.-H. Lee, and S. J. Pearton, Appl. Phys. Lett. **106**, 132101 (2015).
[43]E. B. Yakimov, P. S. Vergeles, A. Y. Polyakov, I.-H. Lee, and S. J. Pearton, Jpn. J. Appl. Phys., Part 1 **55**, 05FM03 (2016).